Inverse design of nonlinearity in energy harvesters for optimum damping

Maryam Ghandchi Tehrani[1*] and S. J. Elliott[1]

[1]Institute of Sound and Vibration Research, University of Southampton,
SO17 1EN, Southampton, UK

Abstract. This paper presents the inverse design method for the nonlinearity in an energy harvester in order to achieve an optimum damping. A single degree-of-freedom electro-mechanical oscillator is considered as an energy harvester, which is subjected to a harmonic base excitation. The harvester has a limited throw due to the physical constraint of the device, which means that the amplitude of the relative displacement between the mass of the harvester and the base cannot exceed a threshold when the device is driven at resonance and beyond a particular amplitude. This physical constraint requires the damping of the harvester to be adjusted for different excitation amplitudes, such that the relative displacement is controlled and maintained below the limit. For example, the damping can be increased to reduce the amplitude of the relative displacement. For high excitation amplitudes, the optimum damping is, therefore, dependent on the amplitude of the base excitation, and can be synthesised by a nonlinear function. In this paper, a nonlinear function in the form of a bilinear is considered to represent the damping model of the device. A numerical optimisation using Matlab is carried out to fit a curve to the amplitude-dependent damping in order to determine the optimum bilinear model. The nonlinear damping is then used in the time-domain simulations and the relative displacement and the average harvested power are obtained. It is demonstrated that the proposed nonlinear damping can maintain the relative displacement of the harvester at its maximum level for a wide range of excitation, therefore providing the optimum condition for power harvesting.

1. Introduction

Nonlinear control can be achieved by introducing nonlinearities in the damping force or stiffness force, to enhance the performance of the system through vibration isolation [1] or energy harvesting [2]. Nonlinear damping has been observed in a significant number of engineering systems such as automotive shock absorbers [3,4], orifices [5], loudspeakers [6], nanoelectromechanical systems such as graphenes [7] and aircraft wings [8]. It has been demonstrated that quasi-linear models can provide a very good approximations to obtain the dynamic response of such systems [9], since nonlinear damping in contrast to nonlinear stiffness does not introduce jump or bifurcation phenomena to the system's response.

Nonlinear damping has also been investigated for the problem of energy harvesting by Ghandchi Tehrani et al [2] to extend the dynamic performance range of the harvester. The system with nonlinear damper can harvest more energy at resonance when driven below its maximum amplitude compared to the system with linear damper.
In this paper, first a model of an energy harvester is provided. The constraint of maximum relative displacement is included in the model. The optimum damping is obtained in order to maintain the amplitude at its maximum level when the base excitation amplitude exceeds its threshold. Then a nonlinear model is fitted to the optimum damping, which is dependent on the amplitude levels. An optimisation is carried out to fit a bilinear model to the variable damping. The bilinear damping model is then validated using time domain simulation.

2. Energy Harvesting with Optimum Linear Damping

A single degree-of-freedom system (spring-mass-damper) shown in Figure 1 is considered, which is subjected to a base excitation, where m is the mass, k is the suspension stiffness, c is a damper, x is the mass displacement, y is the base displacement and z is the relative displacement between the mass of the harvester and the base . The system is harmonically excited at resonance frequency ω_n and the amplitude Y. The damping c consists of an internal inherent damping, c_I, which is a damping loss and an additional shunt damping, c_A, that harvests power.

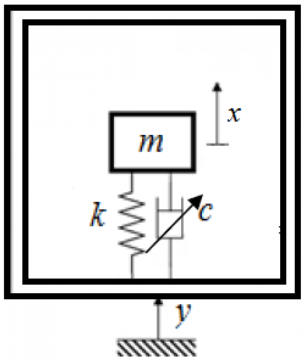

Figure 1: Single degree-of-freedom base excited system with a variable damper

The governing dynamic equation can be written as:

$$m\ddot{z} + (c_I + c_A)\dot{z} + kz = -m\ddot{y}. \tag{1}$$

For harmonic base excitation,

$$y = Y\cos(\omega t), \tag{2}$$

The fundamental component of the relative displacement is assumed to be,

$$z == Z\cos(\omega t - \phi), \tag{3}$$

where, Z is the amplitude of relative displacement and ϕ is the phase shift between z and y .

At resonance, ω_n, the relative displacement can be obtained from [10],

$$Z = \frac{m\omega_n Y}{c_A + c_I}. \tag{4}$$

The relative displacement of the harvester at resonance depends on the damping value and the base excitation amplitude. The device has a maximum relative displacement $Z_{\max}$ due to its physical throw limit. For a fixed value of c_A and c_I, and at a particular base excitation amplitude $Y_{\max}$, the harvester can reach its maximum relative displacement.

For base excitation below $Y_{\max}$, the shunt damping, c_A, can be adjusted such that the relative displacement is at its maximum and the device operates at its optimum condition. The optimum quasi-linear damping, which is level dependent, can be found from,

$$c_A = \frac{m\omega_n Y - c_I Z_{\max}}{Z_{\max}}. \quad (5)$$

The average harvested power can be obtained from the shunt damping and the relative displacement as,

$$P_{\text{ave}} = \frac{1}{2} c_A \omega_n{}^2 Z^2 \quad (6)$$

The internal damping dissipates energy and therefore is not included in the harvested energy. Using Eq. (4) for the relative displacement, we can obtain the average harvested power in terms of the base excitation amplitude.

$$P_{ave} = \frac{1}{2} \frac{c_A}{(c_A + c_I)^2} m^2 \omega_n^4 Y^2. \quad (7)$$

The average harvested power is maximised with respect to the shunt damping $\left(\frac{\partial P_{ave}}{\partial c_A} \right) = 0$, which results in $c_A = c_I$ [10], assuming that this is less than that required to limit the throw in Eq. (5).

3. Numerical Simulation

The simulation parameters for the single degree-of-freedom harvester are:

$$m = 1\text{kg} \quad k = 4\pi^2 \text{ N/m}, \; c_I = 0.1\text{Ns/m}, \; Z_{\max} = 1\text{m},$$

so that the natural frequency of the system is 1 Hz. If a fixed shunt damper is used, its value needs to be $c_A = 1Ns/m$ in order to limit the throw to $Z_{\max} = 1m$, at the assumed maximum excitation amplitude, $Y_{\max}$, of 0.1751m. When the base excitation amplitude reduces, the relative displacement then reduces linearly, as can be seen in Figure 2(a) with blue dashed line.

From the power equation, lower values of shunt damping would result in higher values of the average harvested power. However, the shunt damping cannot be too small, since the relative displacement cannot exceed the physical threshold, so that a level-dependent damper is used, which has a value of 1Ns/m for $Y_{\max}$, but reduces linearly to maintain the throw at $Z_{\max}$ until its value is equal to the optimum mechanical load of 0.1Ns/m, below about 0.03m.

The average harvested power using the fixed damping, $c_A = 1Ns/m$, and the amplitude dependent damping are plotted in Figure 2(c).

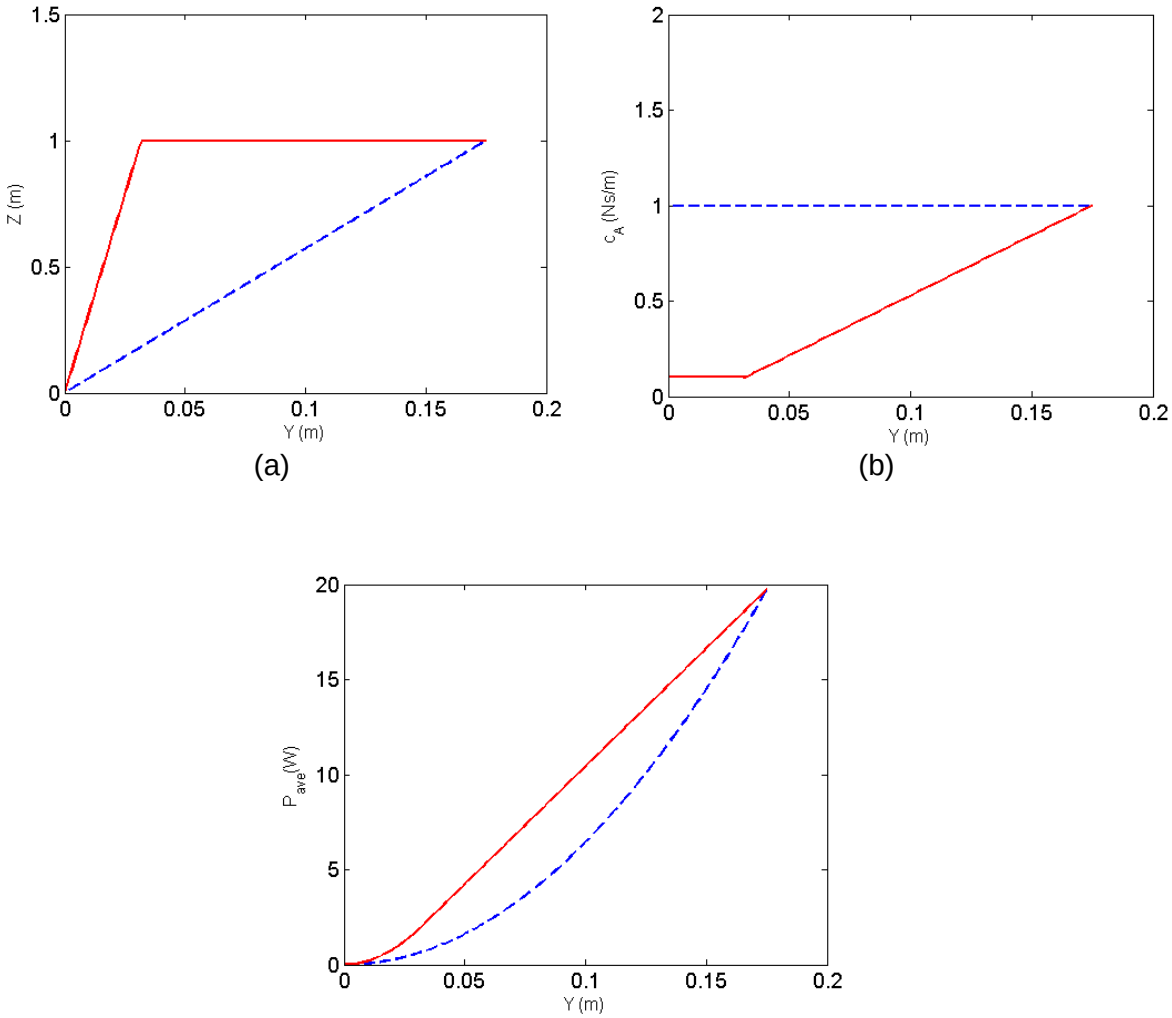

Figure 2: (a) Relative displacement, *Z*, (b) shunt damping, c_A, and (c) average harvested power, P_{ave}, as a function of the base excitation amplitude, *Y* for the quasi-linear model; The optimum linear shunt damper is marked with red solid line and fixed shunt damper is marked with blue dashed line

In order to implement the quasi-linear damper in practice, the damping of the harvester needs to be adjusted based on the amplitude of the base excitation. One approach is to synthesize a nonlinear damper by using a shunt with a static nonlinearity that provides the required variation of quasi-linear damper with level. A bilinear model can be considered, which describes the damping force in terms of the relative velocity, where the relative velocity is $2\pi\ m/s$ for the maximum throw. For the harvester with the variable damper, the damping force changes linearly with the velocity until it reaches the limit of $2\pi\ m/s$ as shown in Figure 3(a). The aim is to fit a bilinear function to this curve. The damping is also shown in Figure 3(b) as a function of the amplitude of the relative velocity. An optimisation will be carried out in the next section in order to synthesize the variable damper with a nonlinear function.

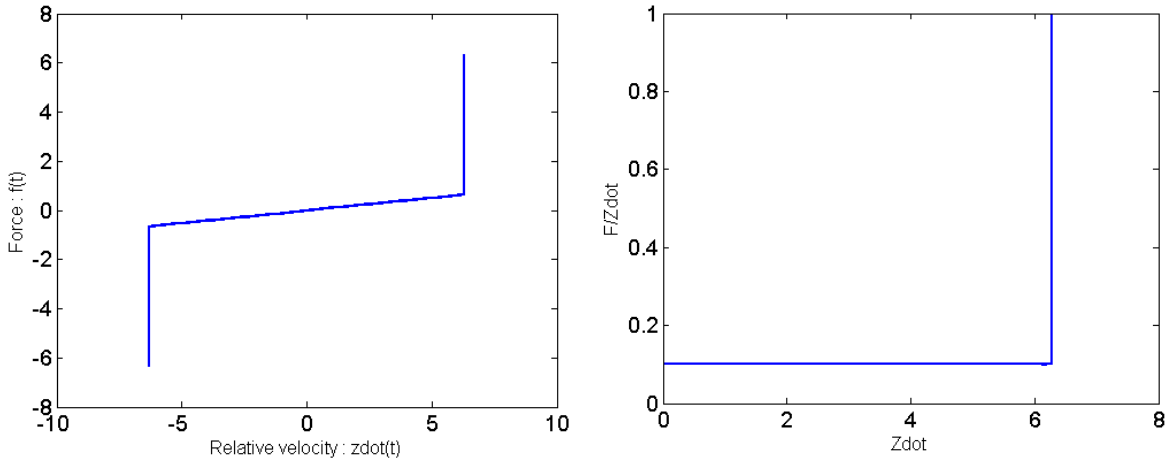

(a) (b)

Figure 3: (a) The damping force versus the relative velocity, (b) the describing function versus the amplitude of the relative velocity

4. Nonlinear Model

In this section, a general nonlinear function between the damping force and the relative velocity is considered as shown in Figure 4(a).

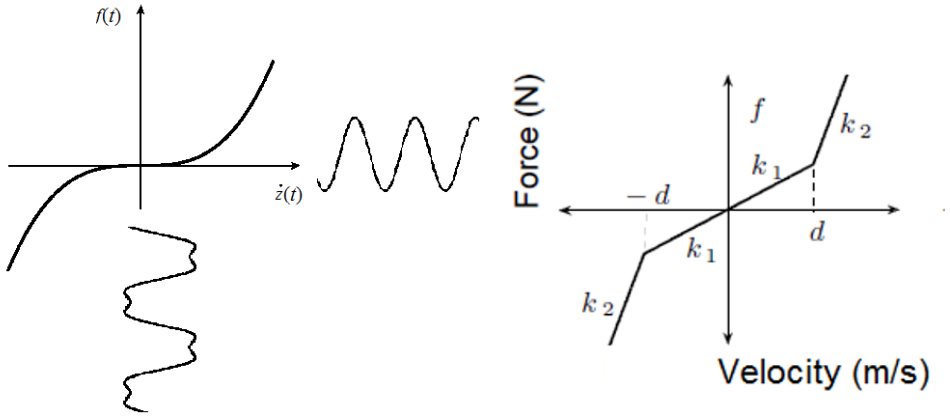

(a) (b)

Figure 4: (a) A general nonlinear function between the damping force and the relative velocity, (b) a bilinear model of damping force

The velocity response is assumed to be harmonic and has an amplitude of $\dot{Z}$ and the fundamental frequency component only. Therefore,

$$\dot{z}(t) = \dot{Z}\sin(\omega t) \tag{9}$$

However, the damping force $f(t)$, is nonlinear and contains the harmonics.

To obtain the amplitude of the damping force, F , at the fundamental frequency, the coefficients of the Fourier series of the nonlinear function are obtained. For example,

$$a_1 = \frac{2}{T}\int_0^T f(t)\cos(\omega t)dt\,, \qquad b_1 = \frac{2}{T}\int_0^T f(t)\sin(\omega t)dt \tag{10,11}$$

The amplitude of the damping force can then be found from $F = \sqrt{a_1^2 + b_1^2}$. The describing function, which is the ratio between the amplitude of the nonlinear force and the amplitude of the velocity at the fundamental frequency, is equal to the level dependent shunt damping c_A.

$$c_A(\dot{Z}) = \frac{F(\omega)}{\dot{Z}(\omega)} \tag{12}$$

If we consider the nonlinear function to be a bilinear model, then the damping force can be written as,

$$\begin{aligned} f(t) &= k_1 \dot{z} \qquad \text{if } \dot{z} \le d \\ f(t) &= k_1 d + k_2(\dot{z} - d) \text{ if } \dot{z} > d \end{aligned} \tag{13}$$

where, k_1 and k_2 are the slopes of the two lines in Figure 4(b) and d is the saturation limit. The describing function of the bilinear model is in the form of [11],

$$c_A(\dot{Z}) = \frac{2(k_1 - k_2)}{\pi}\left(\sin^{-1}\left(\frac{d}{\dot{Z}}\right) + \frac{d}{\dot{Z}}\sqrt{1-\left(\frac{d}{\dot{Z}}\right)^2} + k_2\right). \tag{14}$$

An optimisation is carried out to find the parameters of k_1, k_2 and d such that,

$$\min\left|c_A(\dot{Z})_{quasi-linear} - c_A(\dot{Z})_{bi-linear}\right| \tag{15}$$

A constraint of positive describing function is also used to achieve sensible parameters. The optimum bilinear parameters are found to be,

$$k_1 = 0.1,\ k_2 = 1000 \text{ and } d = 2\pi \tag{16}$$

The instantaneous bilinear damping force is shown in Figure 5(a) together with the variation of its quasi-linear damping with level. There is a good agreement between the quasi-linear and the bilinear damping model. The describing function of the bilinear model, Eq.(14) is in good agreement with the quasi-linear damping.

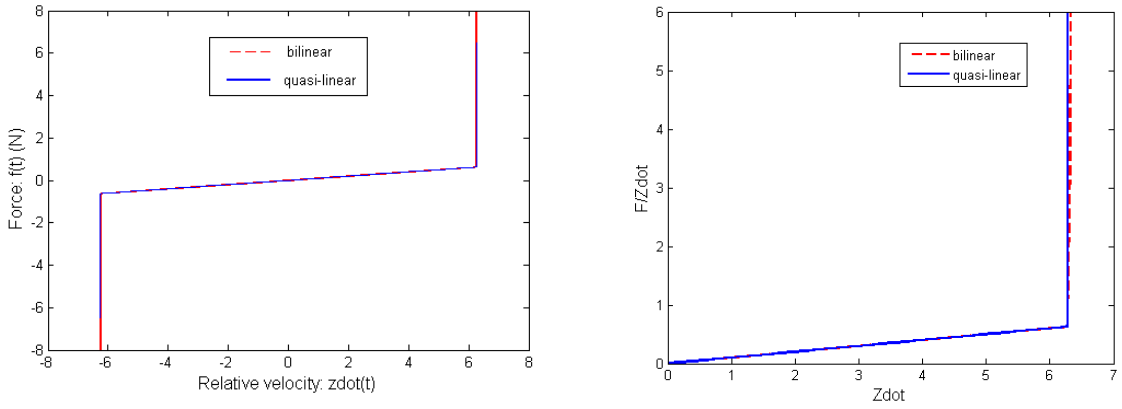

(a) (b)

Figure 5: (a) The instantaneous bilinear damping force versus the relative velocity, (b) The analytical describing function versus the amplitude of the relative velocity; quasi-linear is marked with solid line and bilinear is marked with dashed line.

5. Time Domain Simulation

The bilinear damper obtained from the optimisation is now used in time-domain simulations and the describing function is plotted for different excitation levels. A state-space model is constructed in Matlab and integrated numerically using ode45,

$$\begin{pmatrix} \dot{z} \\ \ddot{z} \end{pmatrix} = \begin{bmatrix} 0 & 1 \\ -\frac{k}{m} & -\frac{f(t)}{m} \end{bmatrix} \begin{pmatrix} z \\ \dot{z} \end{pmatrix} + \begin{pmatrix} 0 \\ -\ddot{y} \end{pmatrix} \tag{15}$$

where, the damping force from Eq.(13) is substituted into Eq. (15) . The amplitude of the base excitation Y is varied from 0 to $2Y_{\max}$ and the response of the nonlinear system is obtained at every amplitude. The instantaneous bilinear function is plotted in Figure 6(a) for two different amplitudes of the base excitation $Y = 0.01m$ and $Y = 0.3m$. For low levels, the response is linear; however for high level of excitation the response is saturated.

The describing function is also plotted using the numerical velocity and damping force in Figure 6(b). There is a slight discrepancy between the two results, since the time data contains harmonics.

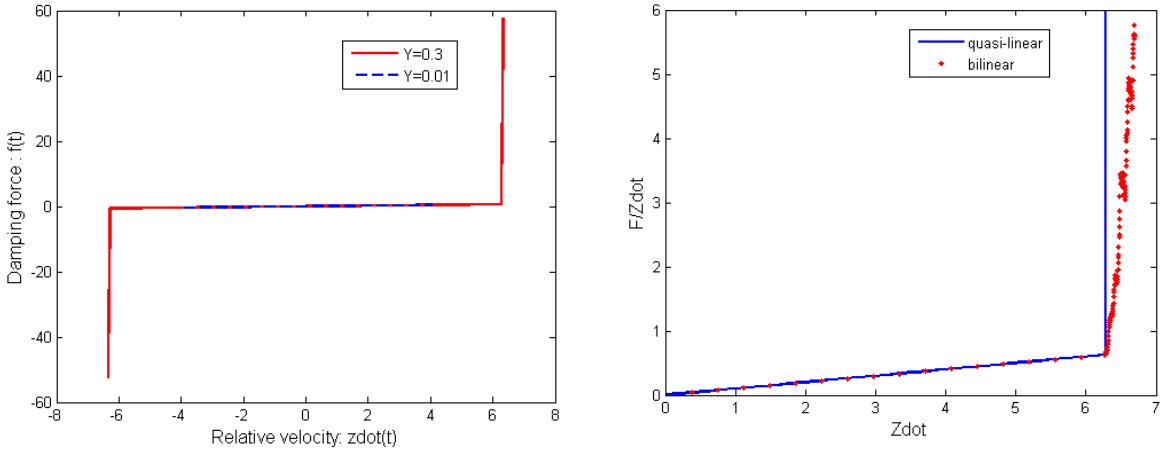

(a) (b)

Figure 6: (a)The bilinear damping force versus the relative velocity from time domain simulation using two different base excitation amplitudes, (b) the numerical describing function (red dotted line) versus the amplitude of the relative velocity compared with the quasi-linear model (blue solid line)

The time histories of the base excitation and the relative velocity are also provided in Figure 8 for two different levels of excitation. For low level, the relative velocity is sinusoidal; however, at high level of excitation, the relative velocity is limited and it does not exceed $2\pi\ m/s$.

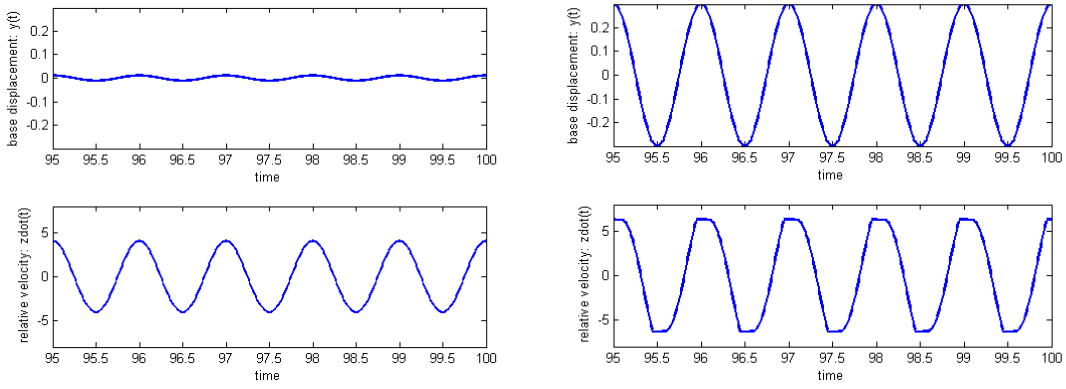

(a) (b)

Figure 7: The time responses for two different base amplitudes (a) $Y = 0.01m$ (b) $Y = 0.3m$

Finally, the relative displacement, the describing function and the average harvested power are calculated using time domain simulation at every excitation amplitude and the plots are shown in Figure 8. The results are in good agreement with the quasi-linear model in Figure 2.

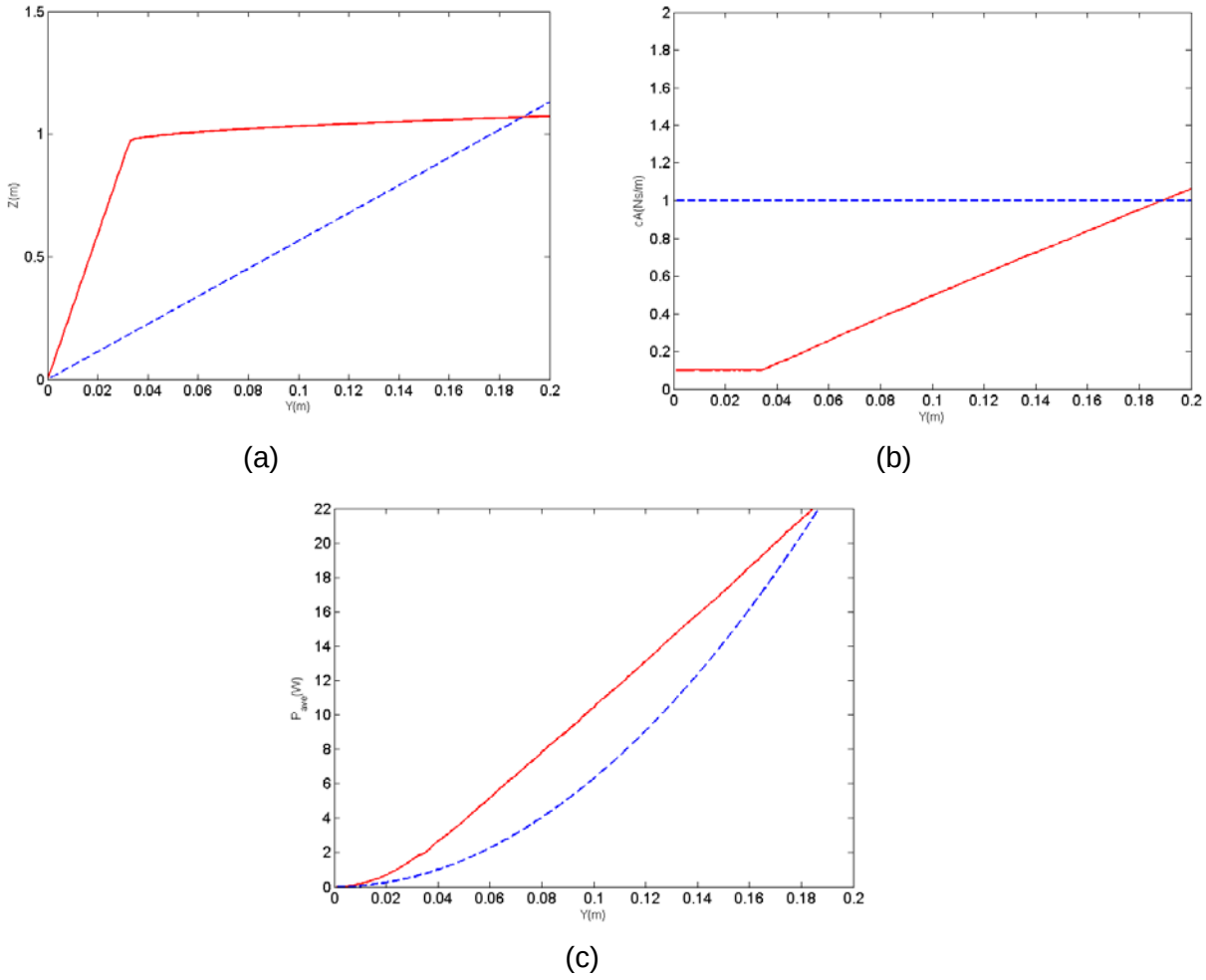

Figure 8:(a) Relative displacement, *Z*, (b) shunt damping, c_A, and (c) average harvested power, P_{ave}, as a function of the base excitation amplitude, *Y* for the bilinear model using time domain simulation; The optimum linear shunt damper is marked with red solid line and fixed shunt damper is marked with blue dashed line

6. Conclusions

This paper has investigated an inverse design of nonlinearity in an energy harvester to achieve optimum damping. When the harvester is excited at an amplitude above its physical limit, the damping can be adjusted to control the displacement level. This results in a level dependent damping at high excitation level. To implement the variable damper, a nonlinear function in the form of bilinear damping is synthesized, which provides a good representation of the linear optimum damper. The bilinear damping is then used in time domain simulation and the response of the system is obtained.

Acknowledgments
Dr Ghandchi Tehrani and Prof Elliott would like to acknowledge the support provided by the EPSRC Engineering Nonlinearity Programme grant (EP/K003836/1).

References

[1] H. Laalej, Z. Q. Lang, S. Daley, I. Zazas, S. A. Billings and G.R. Tomlinson, 2012, Application of nonlinear damping to vibration isolation: an experimental study, *Nonlinear Dyn, 69*,409-421. (DOI: 10.1007/s11071-011-0274-1)

[2] M. Ghandchi Tehrani and S.J. Elliott, 2014, Extending the dynamic range of an energy harvester using nonlinear damping, *Journal of Sound and Vibration,333(3),* 623-629. (DOI: 10.1016/j.jsv.2013.09.035)

[3] J. Wallaschek, 1990, Dynamics of nonlinear automobile shock-absorbers, *International Journal of Non-linear Mechanics, 25(2/3),* 299-308. (DOI: 10.1016/0020-7462(90)90059-I)

[4] C Surace, K. Worden and G.R. Tomlinson, 1992, On the non-linear characteristics of automotive shock absorbers, *Proceedings of the Institution of Mechanical Engineers, IMechE, Part D: Journal of Automobile Engineering, 206,* 3-16. (DOI: 10.1243/PIME_PROC_1992_206_156_02)

[5] U. Ingard and H. Ising, 1967, Acoustic nonlinearity of an orifice, *The Journal of the Acoustical Society of America, 42(1),* 6-17. (DOI: 10.1121/1.1910576)

[6] W. Klippel, 2013, Nonlinear damping in micro-speakers, *Conference on Acoustics, AIA-DAGA, Merano, Italy*.

[7] A. Eichler, J. Moser, J. Chaste, M. Zdrojek, I. Wilson-Rae and A. Bachtold, 2011, Nonlinear damping in mechanical resonators made from carbon nanotubes and graphene, *Nature Nanotechnology, 6,* 339-342. (DOI:10.1038/nnano.2011.71

[8] A. Fellows, T. Wilson, G. Kemble, C. Havill and J. Wright, Wing box nonlinear structural damping, *IFASD-2011*-11.

[9] S. J. Elliott, M. Ghandchi Tehrani and R. S. Langley, Nonlinear damping and quasi-linear modelling, *Phil. Trans. R. Soc. A, 2015, 373*: 20140402, 1-30.

[10] N. G. Stephen, On energy harvesting from ambient vibration, *Journal of Sound and Vibration,* 293 (2006) 409-425.

[11] J. E. Gibson, Nonlinear automatic control, *McGraw-Hill, 1963*.